Chapter 2

Development of mussel mimetic gelatin-based adhesive hydrogel for wet surfaces with self-healing and reversible properties

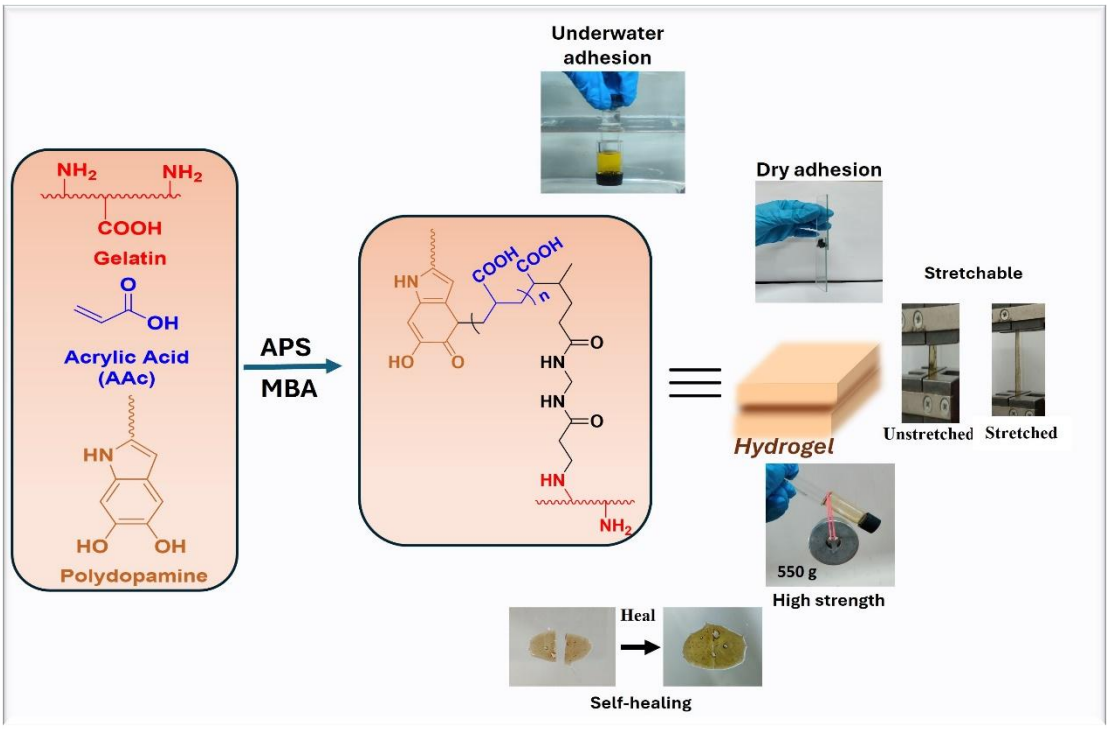

This chapter focuses on the synthesis of an adhesive hydrogel possessing substantial mechanical strength. It also explores the adhesive properties of this hydrogel on various surfaces, under both dry and submerged conditions. In addition, it also highlights hydrogel's inherent self-healing abilities.

Parts of this thesis work are published as:

Ahmed, A., Nath, J., Baruah, K., Rather, M.A., Mandal, M. and Dolui, S.K. Development of mussel mimetic gelatin based adhesive hydrogel for wet surfaces with self-healing and reversible properties. ***International Journal of Biological Macromolecules***, 228:68-77, 2023.

2.1 Introduction

Gelatin-based hydrogels have found numerous applications in various biomedical fields including cell adhesion. Gelatin contains arginine-glysine-aspartic acid (RGD) sequence which helps promote cell adhesion and are also suitable for cell remodeling. Moreover, gelatin-based hydrogels are easily degradable, possess no toxicity, and can be tuned with multifunctional properties, making them an ideal candidate as an adhesive hydrogel. Although numerous adhesives have been developed and found applications in our day-to-day life, but achieving adhesion between two wet surfaces is still challenging. Since water molecules on the surface restrain the two adhering surfaces from coming closer thereby impeding the formation of physical and chemical bonds between the adhesives and the wet surface. Therefore, adhesives that can withstand wet environments caused by moisture, underwater applications, and body fluids are very essential and indispensable materials in many fields mostly in biomedical areas which include tissue engineering, wound healing, biomedical implants, sealants in surgery [1-4]. Therefore, many researchers around the world have shifted their focus toward the adhesive mechanism in nature found in wet and underwater environments. Examples include the toepad of tree frog, caddisfly larva, suction cup of octopi, and adhesive protein in mussels, barnacles, snails, slugs, and sandcastle worms which hang on to the rough surfaces (both hydrophilic and hydrophobic) even under diverse wet conditions [5-8]. As discussed in Chapter 1, the mussel-inspired adhesives are the most widely studied as wet adhesives. The adhesive protein they contain is 3,4-dihydroxyphenylalanine (DOPA) most commonly known as dopamine (Figure 2.1) and their adhesion property is mainly attributed to the presence of catechol moiety which undergoes multiple non-covalent interactions such as H-bonding, π-π interactions, and cation-π interactions with different substrates. These interactions also contribute to the self-healing nature of the dopamine molecule. The long-term adhesive properties of dopamine are due to the redox balance between quinone and catechol groups [9]. Intrigued by this, considerable research has been carried out for synthesizing hydrogel-based adhesives for wet surfaces by emulating the use of the 3,4-dihydroxyphenylalanine group [10-14]. The factors behind the superior nature of the hydrogel-based wet adhesives over traditional wet adhesives include its hydrophilicity which induces a strong capillary adhesion between two wet surfaces. They can also absorb a large amount of water thereby allowing the two adhering surfaces to make closer contact.

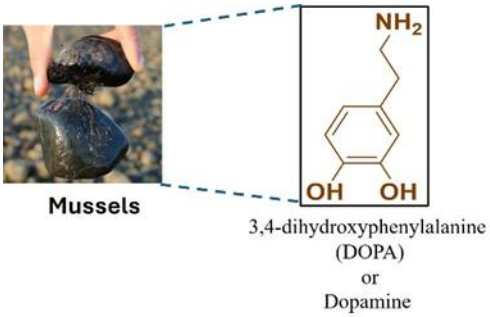

Figure 2.1 Molecular structure of dopamine

Moreover, their close resemblance to that of natural tissue enables their use in a wide range of medical applications including drug delivery, bio-patch, bio-ink, and regenerative medicine [15-19]. Although the crosslinking mechanism of dopamine are not fully understood, it is suggested that oxidation of DOPA to DOPA-quinone or DOPA-semiquinone may lead to crosslinking via radical mechanism with other DOPA residues or with amine via Michael-addition reaction [20-23]. However, the use of oxidant in the synthesis of an adhesive hydrogel is a crucial factor in the formation of polydopamine. Since the oxidative agents such as $FeCl_3$, $NaIO_4$, H_2O_2, etc often oxidizes the catechol group rapidly, leading to overoxidation which eventually retarded the polymerization process, and also the lack of a sufficient number of catechol groups results in poor adhesiveness and limited reusability [24,25].

In addition, the toxicity of the metal is also a major concern for its applicability in biomedical fields. Therefore, fabrication of a hydrogel-based adhesive is one of the key hurdles in achieving tough adhesion between hydrogels and wet surfaces. Han *et al.* designed a tough polydopamine-polyacrylamide (PDA-PAM) single network hydrogel with superior self-healing ability and tissue adhesiveness. They do so by preventing the over-oxidation of dopamine to maintain enough free catechol groups [26]. Again Chen *et al*. composed a tissue adhesive hydrogel based on dopamine and poly(γ-glutamic acid) for local hemostasis application. These hydrogels exhibited stronger tissue adhesive strength as compared to traditionally used clinical fibrin glue [27]. Rao et. al developed a tough hydrogel that shows great underwater adhesion to diverse substrates. The fast and strong adhesion was obtained by combining hydrogels with dynamic ionic and hydrogen bonds and bio-inspired surface drainage architecture. It is desired to obtain

multifunctional hydrogel with high stretchability, reversibility, self-healing, and tough mechanical properties along with strong and dynamic adhesion to diverse substrates.

In this chapter, we have designed a facile method to synthesize a bioinspired hydrogel-based adhesive with high mechanical strength, self-healing properties, and reversibility. Here, gelatin is considered as the main material of the adhesive hydrogel. But as the mechanical strength of physically crosslinked gelatin-based hydrogel is poor, it is modified with poly(acrylic acid) to form double network (DN) adhesive hydrogel. Afterward, the dopamine molecule was grafted to the gelatin-co-poly(acrylic acid) backbone to enhance the wet adhesive and other functional properties of the hydrogel [28,29]. Here, the addition of acrylic acid (AAc) not only improved the mechanical strength of the polymeric hydrogel but also played a significant role in maintaining the adhesive property of the hydrogel. The developed hydrogel is then studied for its adhesive strength in both dry and wet conditions. The mechanical properties along with self-healing properties and blood compatibility of the hydrogel are also studied.

2.2 Experimental section

2.2.1 Materials

Acrylic acid (AA) and N,N/-methylenebis(acrylamide) (MBA) were purchased from Sigma Aldrich. Gelatin, from porcine skin (type A) was purchased from Himedia. Dopamine hydrochloride (DA) was purchased from Alfa Aesar. Sodium hydroxide and ammonium peroxodisulfate (APS) were obtained from Merck. Deionized water was used during the experiment for preparing various solutions. All the reagents used were of analytical grade and were used as received.

2.2.2 Synthetic procedures

Synthesis of polydopamine: Polydopamine (PDA) formation can be achieved through oxidation of DA molecules by alkali solution by following the procedure previously reported by Lu Han with little modification. Here a fixed amount of dopamine powder was dissolved in 2ml aq. NaOH solution by maintaining the pH at 10. The solution is then stirred in air atmosphere for 15 minutes or until the appearance of a slight brownish colour of the solution.

Synthesis of hydrogel: The synthesis of hydrogel was carried out by free radical polymerization in distilled water. Initially, 1g of gelatin powder were dissolved in 15 ml

of double distilled water in a round bottom flask at 55 °C. The mixture was then stirred for 30 minutes for the complete dissolution of the gelatin molecule. Afterward, 0.75 ml of acrylic acid monomer was added to the gelatin solution followed by addition of crosslinker MBA. The whole reaction mixture was deoxygenated by purging nitrogen atmosphere for 15 minutes. Finally, the polydopamine solution along with initiator APS was added to the reaction mixture, and the temperature was raised to 70 °C. After stirring for 1 hour, the reaction mixture turned to a brown-coloured gel. The hydrogel thus obtained was washed with distilled water to remove the residual monomer. The detailed composition of the hydrogel is shown in Table 1.

Table 2.1. Detailed composition of the hydrogel with varied compositions of DA

Hydrogels	*Gelatin (g)*	*AAc (ml)*	*DA (wt%)*	*APS (wt%)*	*MBA (wt%)*
DA1	1	0.75	1	5	0.8
DA2	1	0.75	2	5	0.8
DA3	1	0.75	3	5	0.8

2.3 Characterization

2.3.1 Fourier transform infrared spectroscopy (FTIR)

The obtained hydrogel sample was first air-dried followed by grinding to small pieces which was then used for FTIR spectral analysis and was prepared with potassium bromide (KBr) pellets and the spectra were recorded between 4000-500 cm^{-1} by using Impact 410 (Nicolet, USA) Fourier Transform Infrared (FTIR) spectrometer and the number of scans was four.

2.3.2 Powder X-ray diffractometry (XRD)

The air-dried and ground hydrogel sample was used for X-ray diffraction (XRD) data, which were recorded using a Rigaku Miniflex X-ray diffractometer (Tokyo, Japan) by employing Cu Kα radiation (λ= 0.1548 nm) at a voltage of 30 kV and 15 mA current and the angle (2θ) was in the range of 10° to 80°.

2.3.3 Scanning electron microscopy (SEM)

The surface morphology of the synthesized hydrogel was studied using a Scanning Electron Microscope (SEM, Model-JSM-6390 LV, JEOL, Japan). Before performing the analysis, the surface of the sample was first coated with Platinum.

2.3.4 Thermogravimetric analysis (TGA)

To analyze the thermal stability of the air-dried hydrogel, Shimadzu TA-60 thermogravimetric analyzer was used. The heating rate was 10 °C/min under the N_2 atmosphere, and the maximum temperature reached up to 600 °C.

2.3.5 X-ray photoelectron spectroscopy (XPS)

XPS analysis of the air-dried and ground samples was done in the 'ESCALAB 220 XL spectrometer using 100 eV and 40 eV constant analyser energies for survey spectra and high-resolution spectra, respectively

2.3.6 Optical microscopic images

Optical microscopic images were recorded by using MOTIC BA310Pol Microscope.

2.3.7 Determination of equilibrium swelling

The equilibrium swelling of the hydrogels were carried out in distilled water and buffer solutions of pH 1.2 and 7.4. For this, a fixed amount of dehydrated samples were immersed in water or buffer solutions and allowed to swell until an equilibrium swelling was reached. The swelling percentage was then calculated by using the formula:

$$\text{Swelling \%} = \frac{W_s - W_d}{W_d} \times 100\%$$

W_s and W_d are the weights of the swollen and dehydrated samples respectively.

2.3.8 *In vitro* Hemocompatibility study

The hemocompatibility study was carried out according to the method reported by Das Purkayastha *et al*., with slight modifications (Das et.al., 2013) [30]. For this, fresh goat blood was collected in a centrifuge tube containing trisodium citrate (3.2%) which was then centrifuged at 2500 rpm at 4 °C for 15 min. The supernatant thus obtained was discarded and the Red blood corpuscles (or erythrocytes) were collected

and washed with phosphate-buffered saline (PBS; pH 7.4) for three times. 10% v/v erythrocyte suspension was prepared in PBS and 1.9 ml of the same was taken in a centrifuge tube containing 2 mg of the samples. 1% Triton and NaCl were taken on a positive and negative control respectively. After the incubation is over, the test tubes bearing samples and suspension were again centrifuged at 40 °C for 15 min at 2500 rpm. By using a UV-Visible spectrometer, the absorbance of the supernatant was recorded at 540 nm.

2.3.9 Mechanical Tests

The tensile test of the hydrogel (ASTM D638) was determined by using Universal Testing Machine (UTM, Zwick, Z010). For the test, the hydrogel samples were cut into pieces with a dimension of 14mm × 0.29 mm (width × thickness). The constant loading rate was set at 5 mm/min. The tensile tests of different samples were carried out by varying the concentration of dopamine. The tensile strength is calculated as:

$$\text{Strength} = \frac{Maximum\ load}{cross\text{-}sectional\ area}$$

2.3.10 Adhesion test

The adhesive strengths (ASTM D638) of the synthesized hydrogels were measured by performing a lap-shear adhesion test on a Universal Testing Machine (UTM, Zwick, Z010) under ambient conditions. For this, hydrogels were applied between two surfaces with a specific bonded area. The lap shear adhesion tests were conducted after a curing time of 24 hours. The adhesive tests were also performed on different substrates such as glass, wood, aluminum sheet, plastic, chicken flesh, and chicken skin by simply pressing the two-surface adhered by the hydrogel and by monitoring the holding capacity of the two bonded surfaces. Similarly, to evaluate the adhesive property under wet conditions, the substrate to be tested were first immersed in water and then glued together with the adhesive hydrogel under water. The adhesive strength is calculated as:

$$\text{Strength} = \frac{Maximum\ load}{Bonded\ area}$$

2.3.11 Self-healing experiment

To evaluate the self-healing property of the hydrogel, the hydrogel sample with a dimension of 22mm × 11mm × 0.8mm (Length × Width × Thickness) was cut into two

halves and then the two halves were brought into contact immediately. The hydrogel shows self-healing behavior within 1 hour. However, the complete healing of the hydrogel was measured by stretching the hydrogel to a maximum after 24 hours. No external stress was applied here. To minimize water evaporation from the hydrogel during the self-healing process, the specimen was kept in a closed vessel.

2.4 Results and Discussion

2.4.1 Design strategy for the synthesis of hydrogel

The synthesis of hydrogel-based adhesive was carried out by following a two-step polymerization process. In the first step, the autoxidation of DA molecules to their reactive quinone form is carried out spontaneously in basic aqueous media by dissolved oxygen. During this step, the color of the solution starts turning from a colorless solution to a pale, brown-colored solution. In a basic medium, dopamine (DA) oxidizes to dopaquinone (DQ) which then undergoes intramolecular cyclization *via* 1,4-Michael addition to form leucodopamine (DL) which oxidizes further to form dopamine chrome (DC) which polymerizes resulting in the formation of polydopamine [31-33].

In the second step, the PDA precursor solution was added to gelatin and AAc solution where grafting of PDA to gelatin and AAc takes place. The solution was then degassed with N_2 gas to eliminate the dissolved oxygen. Polymerization was further initiated by adding free radical initiator APS. On heating, APS decomposes to form sulfate anion radical which then attacks the double bond on the acrylate monomer and also abstracts hydrogen from the gelatin side chain to form the corresponding radical. Here the addition of AAc minimized the further oxidation of catechol groups and thereby preserving the adhesive property of the catechol group [34,35]. Moreover, the cationic $–NH_2$ group of gelatin crosslinked covalently with oxidized quinone resulting in interfacial binding. The end vinyl group of the crosslinking agent MBA reacts with the polymer chain to give the final crosslinked hydrogel. The plausible mechanism of hydrogel formation is shown in Scheme 2.1. Hydrogel with different concentrations of DA, initiator, and crosslinker was prepared to study their effect on swelling. The hydrogel thus formed showed excellent adhesion to various surfaces. The hydrogel retains its adhesive property even after multiple adhesions and after many times of soaking and rinsing methods. Moreover, the DA molecule, which is responsible for endowing the self-healing property of the hydrogels, enables the hydrogel to recover

spontaneously from damage. This is mostly due to the presence of catechol –OH group which allows the H-bond formation.

The successful graft of polymerized dopamine on the backbone of the gelatin-co-poly(acrylic acid), has been established by performing a comparative study of hydrogel with and without dopamine.

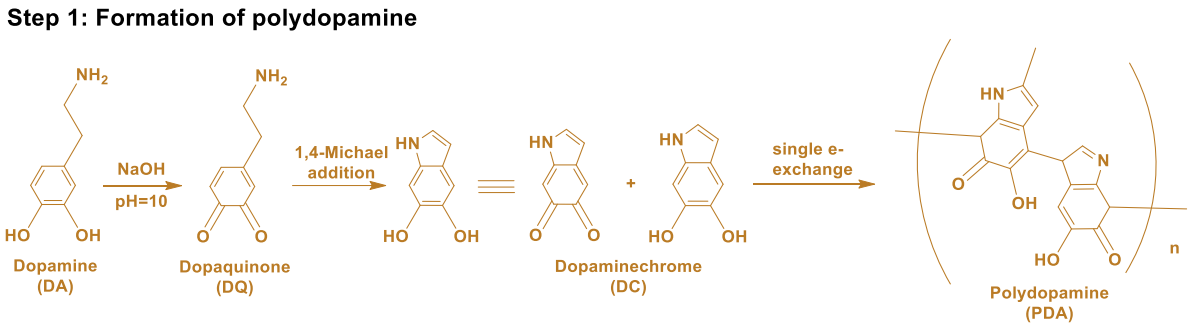

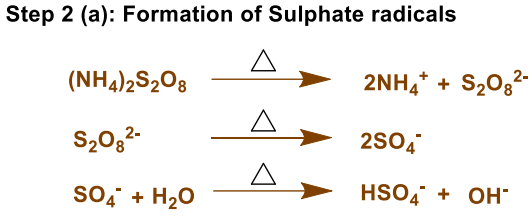

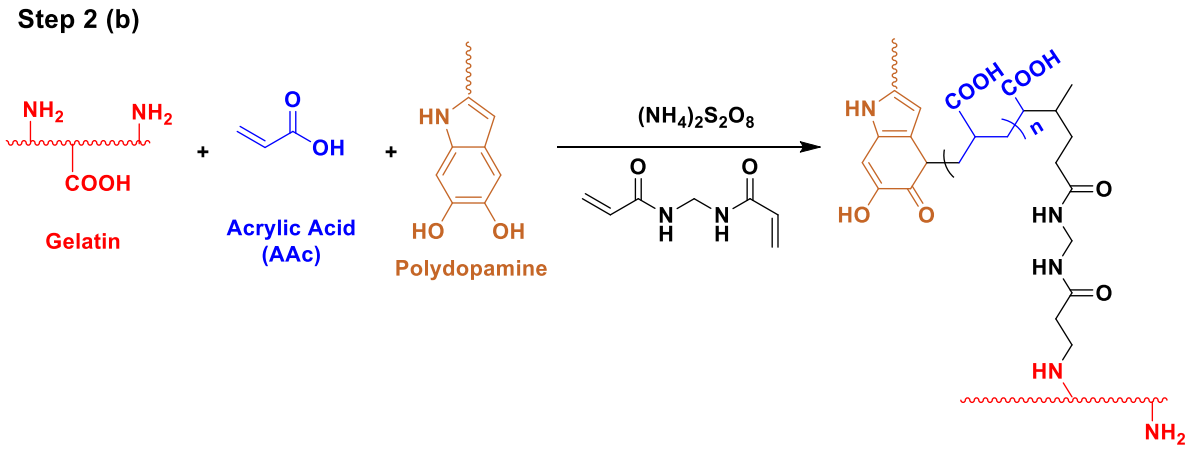

Scheme 2.1. Plausible mechanism involved in the formation of hydrogel

2.4.2 FTIR analysis

The FTIR spectra of the monomers and the prepared hydrogels are shown in Figure 2.2 (a), (b) respectively. For pure gelatin, the characteristic peak at 3435 cm^{-1} is attributed to the NH stretching of the amide group. The CH group of the gelatin is identified from the peak at 2923 cm^{-1}. Again, a sharp peak at 1640 cm^{-1} arises from C=O

stretching vibration. The peak at 1238 cm^{-1} is caused by the C–N stretching vibration of N–H amide in-plane bending vibrations. Again, from the spectral data of AAc, the peak at 3451 cm^{-1} and 2921 cm^{-1} are attributed to the O–H stretching vibration and C–H vibrations respectively. The peak which appeared at 1632 cm^{-1} and 1721 cm^{-1} are assigned to C=C and C=O vibration respectively. The peak at 1409 cm^{-1} is due to the O-H bending vibration. Similarly, the spectral data of dopamine hydrochloride shows a broad and strong band in the 3000-3400 cm^{-1} region revealing the intermolecular hydrogen oscillations on (aromatic) O–H stretching vibrations. Here the peak between 2750 cm^{-1} and 2250 cm^{-1} emerges due to N–H vibration, showing the NH_2 functionality. The sharp peaks that appear below 1700 cm^{-1} are attributed to aromatic C=C and C-H bonds. By comparing the FTIR spectra of the synthesized polymer hydrogel with the monomers, it was found that a broad and weak peak in the range of 3000-3500 cm^{-1} is due to the overlapping of O–H and N–H stretching vibrations. Here the peak at 2925 cm^{-1}, which appears due to the vibration of the C–H group in the methylene group becomes stronger and sharper. This indicates that the carbon-carbon double bond becomes saturated after polymerization. Again, the peak at 1639 cm^{-1} has become broader which is due to the overlapping of stretching vibration of C=C and N–H bending vibration indicating the incorporation of catechol moiety within the hydrogel. Moreover, the peak at 1164 cm^{-1} is due to the C–N stretching vibration of the amine group.

Again the FTIR spectra of (i) dopamine-grafted gelatin-co-poly(acrylic acid) hydrogel and (ii) gelatin-co-poly(acrylic acid) hydrogel are shown in Figure 2.2(c). From the spectra, the peak around 3000-3500 cm^{-1} in dopamine-grafted hydrogel is broader compared to that in the hydrogel without dopamine which is due to the intermolecular hydrogen bonding thereby depicting the incorporation of the catechol group. Again, the peak at 1635 cm^{-1} has become broader in Figure 2(c)(i) which might be due to the overlapping of stretching vibration of C=C and N-H bending vibrations. A small peak around 1501 cm^{-1} emerges in Figure 2(c)(i) which might be due to C=C aromatic stretching vibration peaks. These small changes in peak intensities and emerging of new peaks must depict the successful incorporation of dopamine within the hydrogel matrix.

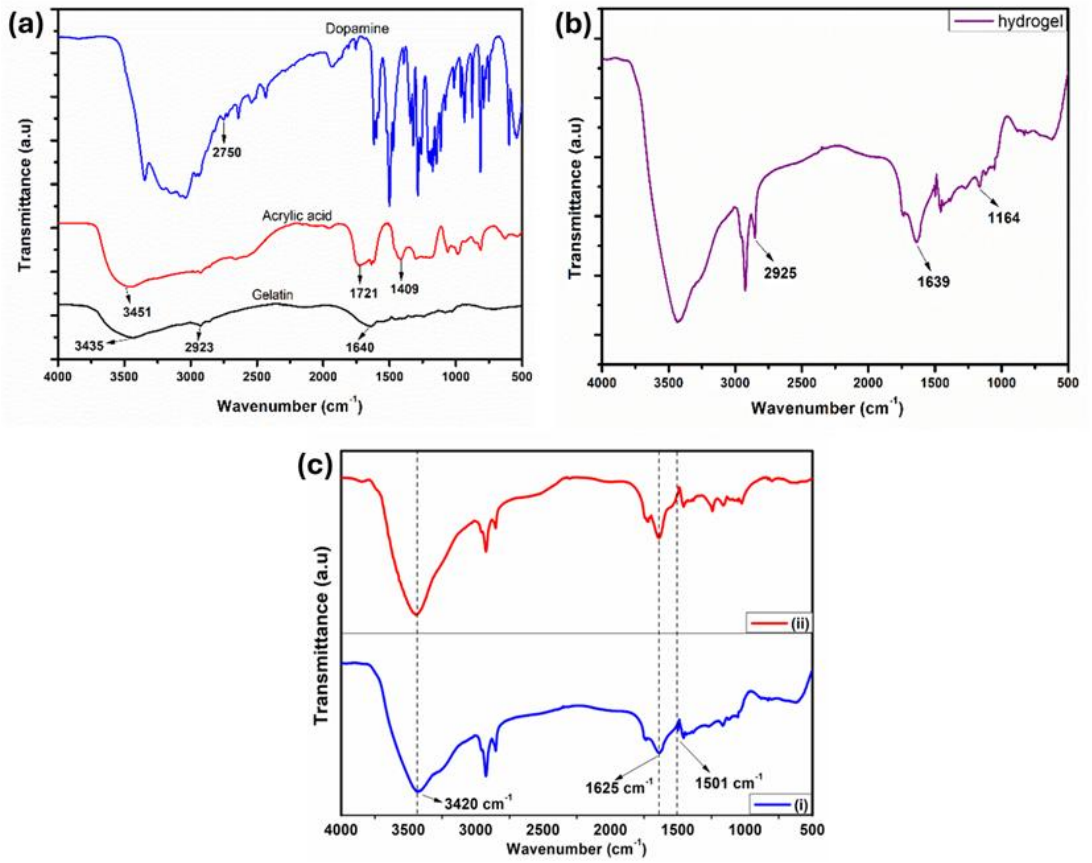

Figure 2.2 FTIR Spectra of (a) monomers, (b) hydrogel; (c) (i) dopamine grafted gelatin-co-poly(acrylic acid) and (ii) gelatin-co-poly(acrylic acid)

2.4.3 XRD

The X-Ray diffraction patterns of gelatin and the prepared hydrogel are compared in Figure 2.3. It is seen that the XRD pattern of pure gelatin showed a broad peak at around $2\theta=20^{o}$ which corresponds to the semi-crystalline nature of the gelatin and a small peak at $2\theta=10^{o}$ might be due to the triple helix structure of gelatin [36,37]. However, in the XRD pattern of the hydrogel, this small peak almost disappeared and the characteristic peak of gelatin at 20^{o} shows some shifts in its position and intensity. This indicates the occurrence of covalent crosslinking among gelatin and other monomer units, thereby destroying the close packing for the formation of regular crystallites.

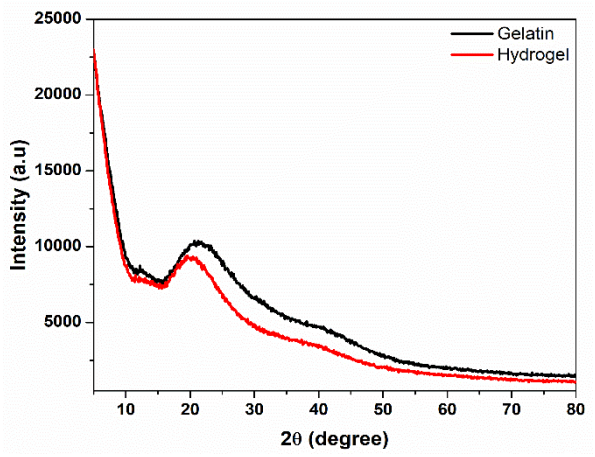

Figure 2.3 XRD Spectra of gelatin and hydrogel

2.4.4 Thermal Degradation Study

The thermogravimetric analysis (TGA) of the synthesized hydrogel was performed to determine its thermal stability. As shown in Figure 2.4, the initial weight loss within the temperature range 100-150 °C with mass loss of 5% is due to the moisture content in the hydrogel matrix. Again, the decomposition of the hydrogel in the range 200-550 °C with a mass loss of 65% is attributed to the thermal degradation of the polymeric chain. However, on increasing the temperature above 500 °C, there occurs no significant mass loss which is due to the presence of crosslinked structure in the hydrogel.

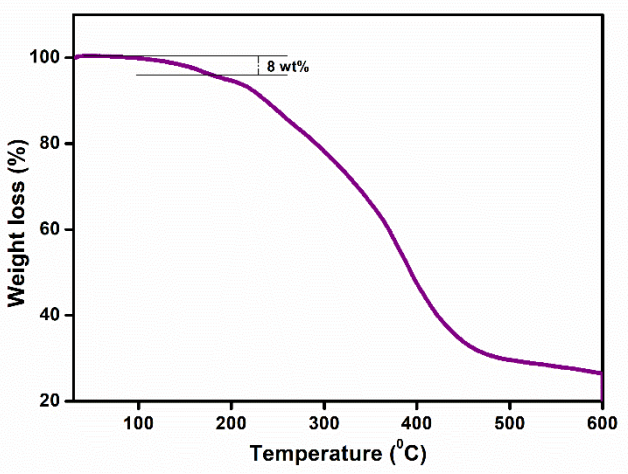

Figure 2.4 TGA spectra of hydrogel

2.4.5 SEM

The morphology of the synthesized hydrogels was studied by using a scanning electron microscope and the images were shown in Figure 2.5. From the given SEM micrograph of the dopa-g-AAc/gelatin (DAG) hydrogel, it has been found that the hydrogel showed a smooth surface. Moreover, the SEM image of the cross-sectional area of the swelled hydrogel i.e. dopa g-AAc/gelatin hydrogel, showed a lamellar structure depicting the incorporation of water molecules within the hydrogel.

The swollen hydrogel as shown in Figure 2.5(a) and (b), refers to the SEM micrograph of air-dried swollen hydrogel, and during air dry, we got a compact structure. Hence, the surface of the hydrogel possesses no visible pores. Instead, some lamellar structures were observed. However, the porous structure can be easily seen when the swollen hydrogel is freeze-dried. The optical microscopic images of the swollen freeze-dried hydrogel are shown in Figure 2.5(c, d).

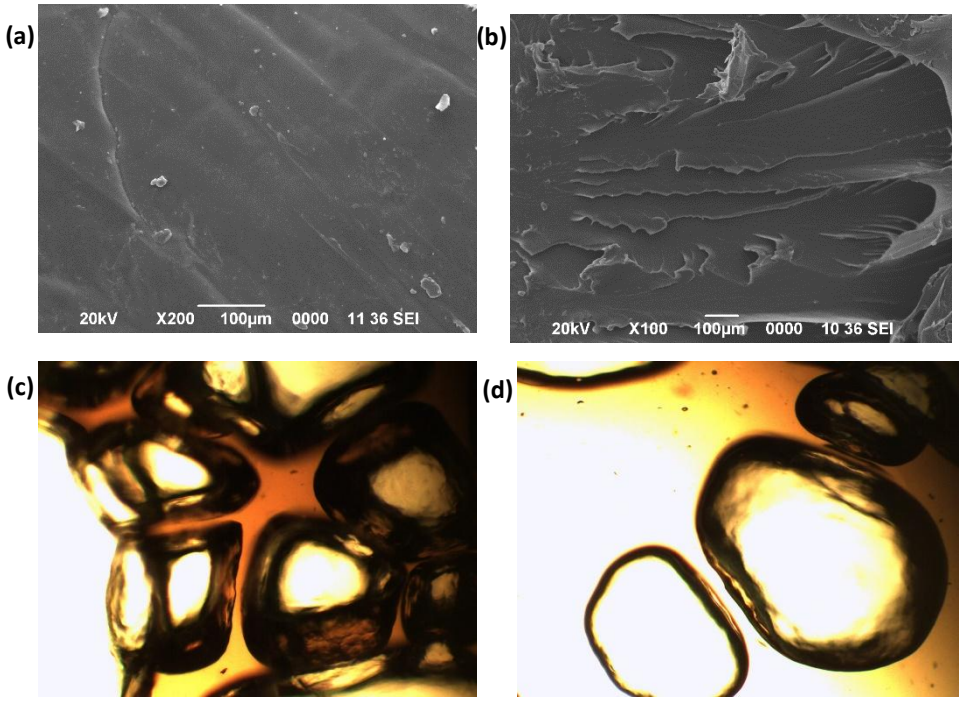

Figure 2.5 SEM morphology of air dried (a) surface of dried hydrogel, (b) cross-sectional area of swelled hydrogel, (c,d) Optical microscopic image of the hydrogel showing porous structure

2.4.6 XPS study

The synthesized hydrogel was further elucidated by XPS analysis. The information for the chemical composition of each element in the hydrogel is shown in Table 2.2. The XPS survey spectra of the hydrogel is shown in Figure 2.6(a), and the high-resolution spectra of C1s, O1s, and N1s were also analyzed as shown in Figure

2.6(b), (c), and (d). The C1s peak is deconvoluted into 4 peaks with binding energies at around 284 eV attributed to C-H and C-C and 285.88 eV and 288.66 eV corresponding to C-O-C and COO^- respectively. Again, the spectra for O1s are deconvoluted into 3 peaks with binding energy 530.55 eV, 531.90 eV, and 532.74 eV, attributed to COO^-, C–O–C, and C=O respectively. For the N1s spectrum, the peak at 400eV is due to C-NH_2. Thus, the XPS study confirms the presence of C–C, COO^-, C–O–C, C=O, and C–NH_2 which further confirms the chemical structure of the hydrogel.

Table 2.2 Chemical compositions of C, N, and O

Atom	*Atomic fraction (%)*
C	75.84
O	21.18
N	2.98

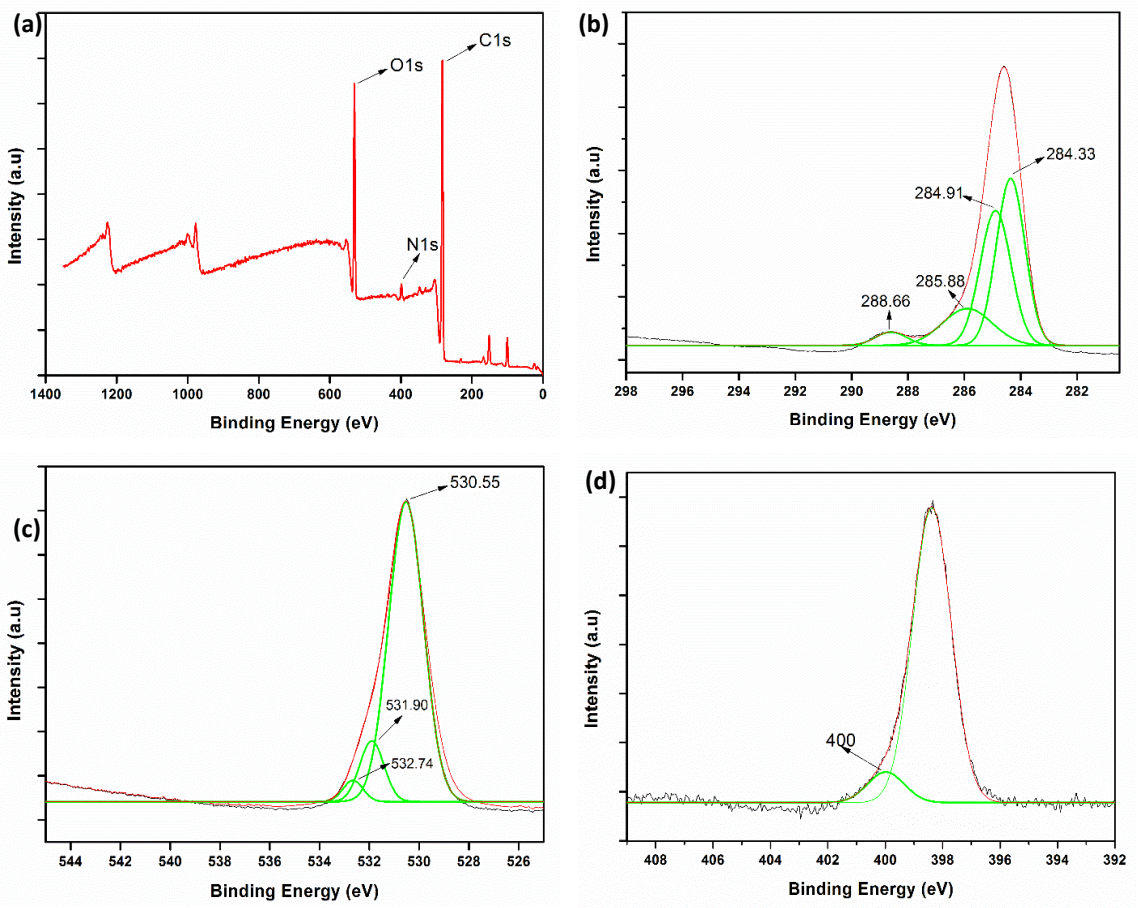

Figure 2.6 (a) XPS survey spectra of the hydrogel, (b) C1s, (c) O1s, (d) N1s spectra

2.4.7 Tensile Test

To study the mechanical properties of the adhesive hydrogel, tensile tests have been performed. The hydrogels are found to be highly stretchable, resilient, and have tough properties. The synthesized hydrogel could be stretched up to 6 times its initial length without any breakage as shown in Figure 2.7(c). After stretching the hydrogel to its maximum, the load is released, and it recovers to its original length spontaneously. On increasing the content of dopamine, there is a sharp increase in the tensile strength of the hydrogel. The tensile strength of a sample containing 1% dopamine is 1.67 MPa and the strength increases from 1.87 MPa to 4.6 MPa on increasing dopamine content from 2 to 3%. Similarly, the elongation at the break of the hydrogel also increases from 66% to 77% and reaches a maximum of 106% with 3% dopamine content. This stress-strain curve is shown in Figure 2.7(a). This elongation at break can be comparable to human skin (60%-75%). This implies that the synthesized hydrogel can be easily applied to the skin to accommodate human movement without tearing. Dopamine increases crosslinking through H-bonding thereby increasing its strength. In stretching this H-bonding disrupts reversibly to accommodate for higher elongation. The Young's modulus is shown in Figure 2.7(b).

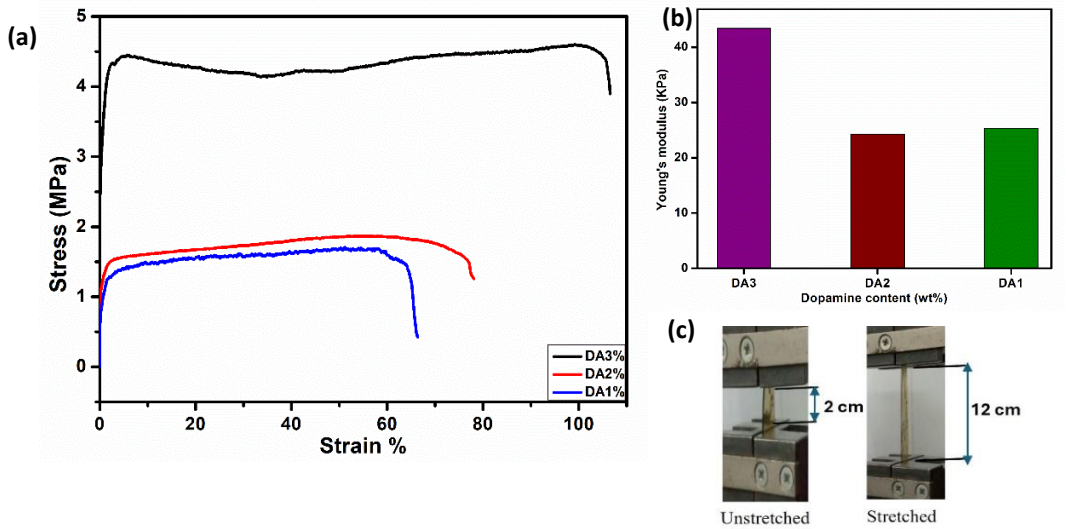

Figure 2.7 (a) Stress-strain curve and (b) Young's modulus of the hydrogel at a dopamine concentration of 3wt%, 2wt%, and 1wt%; (c) Digital photograph of the hydrogel showing unstretched and stretched hydrogel

2.4.8 Adhesion study

In our study, we have found that synthesized hydrogel shows excellent adhesion to almost all surfaces including both hydrophobic and hydrophilic areas. The adhesive

tests were performed on surfaces like human skin, glass slides, aluminum sheets, PTFE, plastic, chicken skin, chicken flesh, etc. (Figure 2.8(a)). The adhesive hydrogel, when applied to glass surfaces, joints with a cross-sectional area of 176.71 mm^2 can hold a weight of 550 g under dry conditions as shown in Figure 2.8(b). The adhesive strength of the hydrogel on various surfaces is evaluated by a lap-shear method. The adhesion strengths for different substrates such as glass, aluminum sheets, and chicken under dry conditions were found to be 112.65 kPa, 26.24 kPa, and 13.2 kPa, respectively, and under submerged conditions, the adhesive strengths were found to be 22.4 kPa, 16.76 kPa, 6.42 kPa, respectively. The hydrogel shows adhesion to surfaces under aqueous conditions. However, the adhesive strength of the hydrogel under aqueous conditions is less compared to their dry adhesion, but it possesses enough strength to hold the two surfaces together. The adhesion under both dry and wet conditions is illustrated in Figure 2.8(d).

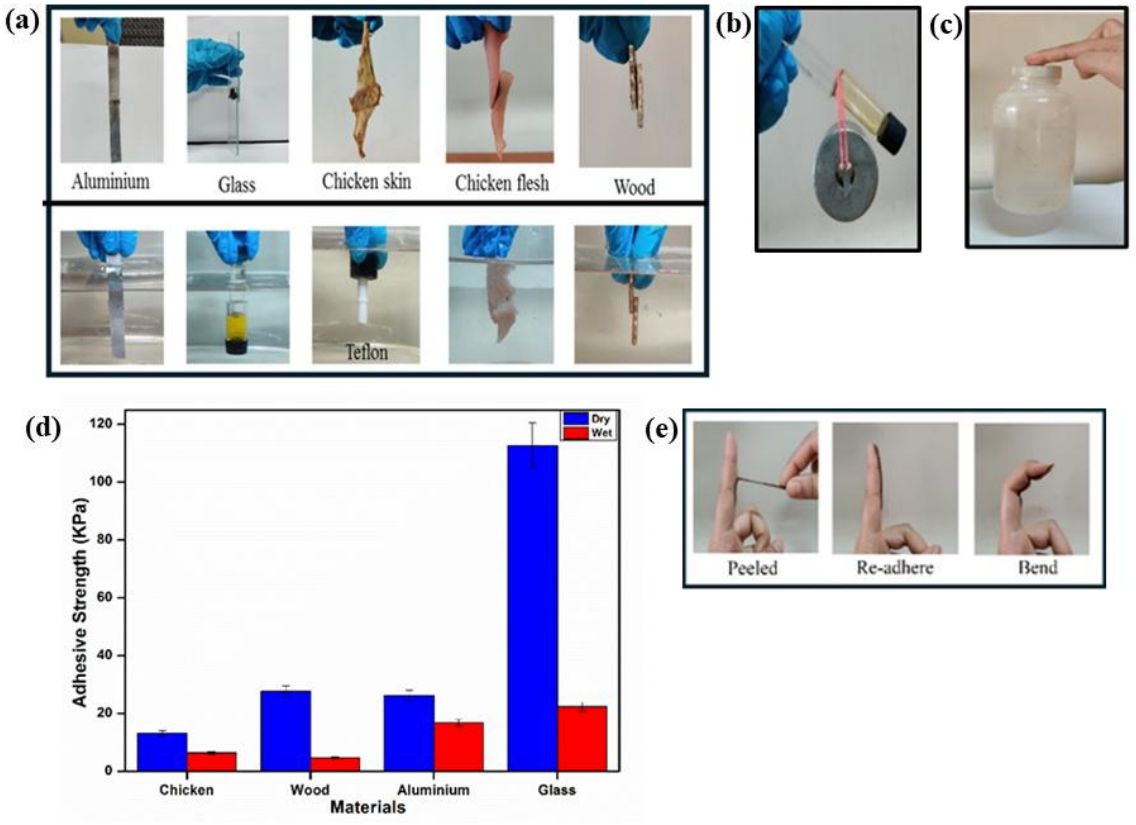

Figure 2.8 Digital photograph of the hydrogel showing (a) adhesion to different materials under both dry (upper) and submerged conditions (lower), (b) hydrogel holding weight of 550 g when adhered to two glass surfaces joints (c) hydrogel lifting a weight of 400g when attached to human skin (d) Adhesive strength of the hydrogel on different materials under both dry and wet conditions (e) repeatable peel-off test on human skin

The adhesive strength of the hydrogel to human tissue is also appreciable. The hydrogel can be adhered easily to human skin without causing any irritation or inflammation to the skin, and can be easily peeled off, thereby leaving no pain or damage to the adhered area. Moreover, a piece of hydrogel with a dimension (13mm × 6mm) when attached to human skin could lift a weight of 400 g as shown in Figure 2.8(c). The hydrogel remains attached to the skin after multiple stretching and bending. The reversible nature of the adhesion can be determined by performing a peel-off test on human skin over 10 cycles as shown in Figure 2.8(e). This cycle ensures the superior and repeatable adhesiveness of the hydrogel even after 10 cycles. Again, the most striking feature of the hydrogel is its ability to retain the adhesive behavior after its swelling to a maximum. It was found that the hydrogel retains adhesion to different surfaces even after swelling to 400% of its original weight. A comparison of the tissue adhesive strength of the synthesized hydrogel to that of the reported adhesive hydrogel is shown in Table 2.3.

Table 2.3 Comparison of the adhesive strength of the synthesized hydrogel-based adhesive under wet condition with previously synthesized hydrogel reported in literature.

Sl. No	*Hydrogel*	*Adhesive strength on tissue (kPa)*	*Reference*
1.	PDA/PAM/XL-MSN	7	[19]
2.	Polyampholyte (PA) hydrogel	5	[38]
3.	poly(d,l-lactide)-poly(ethylene glycol)-poly(d,l-lactide) (PLEL)	5	[39]
4.	PEG-D hydrogel	7.8	[31]
5.	PAM-PEI hydrogel	7	[40]
6.	HA-DA/rGO	6	[41]
7.	PDA@GelMA	2.75	[42]
8.	Dopa-g-Gel/Acc hydrogel	6.5	Present work

2.4.9 Self-healing property

The synthesized hydrogel shows good self-healing property as shown in Figure 2.9(a), and the tensile strength of the self-healed hydrogel is shown in Figure 2.9(b). The self-healing ability of the hydrogel is better understood from the mechanistic point of view as shown in Figure 2.9(c). Since mussel-inspired hydrogel often shows self-healing ability because of the presence of diverse functional groups such as catechol and amine group in the polymeric chain which form multiple non-covalent interactions like H-bonding, cation-π, or π-π interactions with amine or thiol group present in various surfaces. These reversible interactions impart the hydrogel with self-healing ability thereby allowing a rapid and effective reconstruction of the broken hydrogel network.

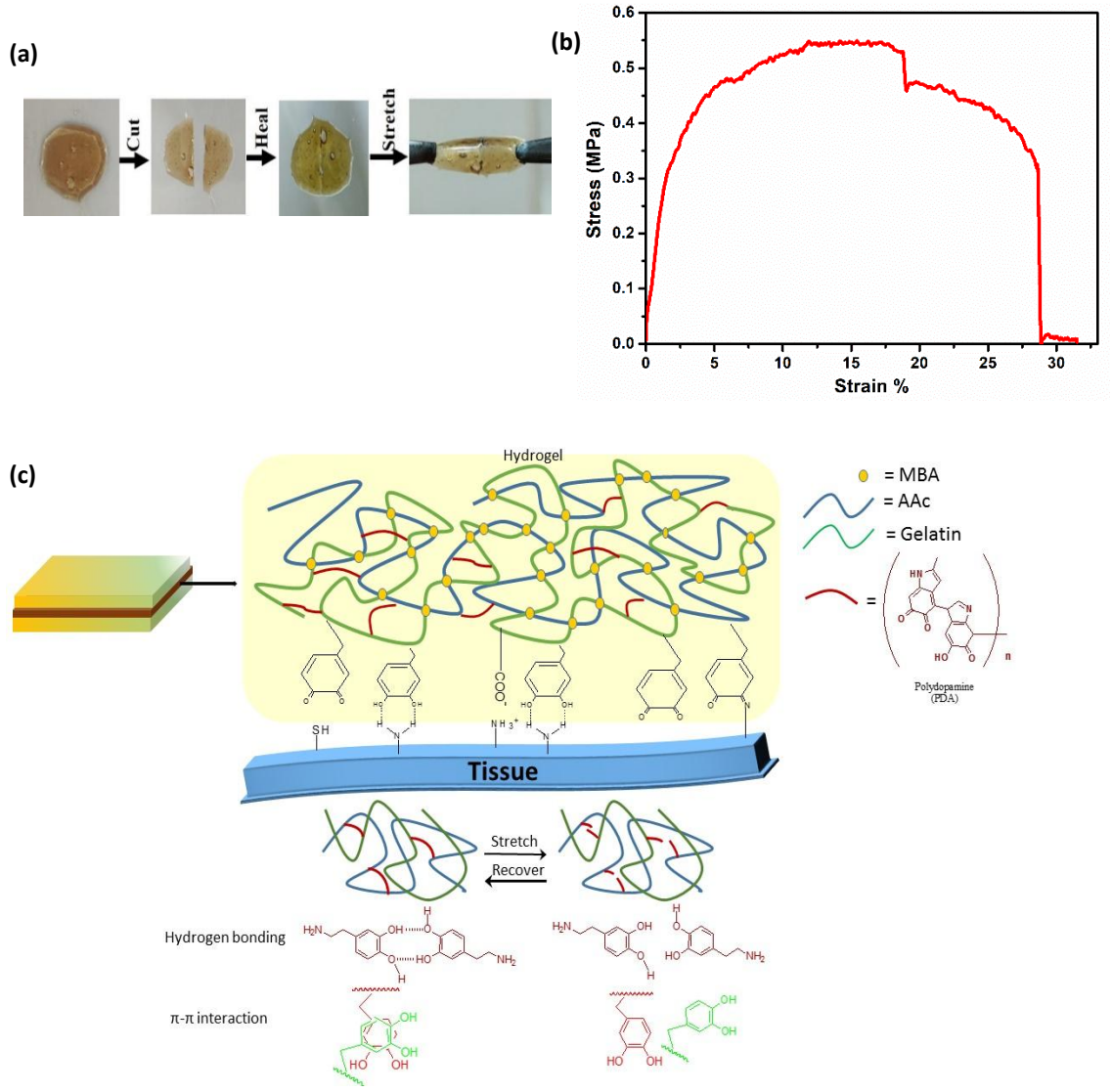

Figure 2.9 (a) Digital photograph of the hydrogel showing self-healing behavior, (b) Stress-strain curve of the self-healed hydrogel, (c) Schematic representation of the adhesive mechanism of the hydrogel to tissue surface

2.4.10 Swelling

The swelling ratio of a hydrogel has a significant impact on hydrogel application, particularly when applied in biomedical fields. To investigate the swelling behavior of synthesized hydrogel, the hydrogels were swelled under distilled water and phosphate buffer solution of pH 7.4. The swelling behavior of the hydrogel is shown in Figure 2.10. It was found that the swelling behavior of the hydrogel at pH 7.4 is higher compared to their swelling at distilled water. This is due to the ionization of the carboxylic group present mostly in acrylic acid. This ionized negatively charged group undergoes repulsion, thereby enhancing the swelling of the hydrogel. Moreover, the swelling ratio of the hydrogel under the same condition is generally related to their cross-linking density. However, no appreciable change in swelling behavior is found by varying the concentration of dopamine. Here the swelling ratio we obtained was relatively low compared to other hydrogels and hence is ideal for its application in the biomedical field, as excessive swelling can cause the surrounding nerves and blood vessels to compress and results in diminishing the adhesive property.

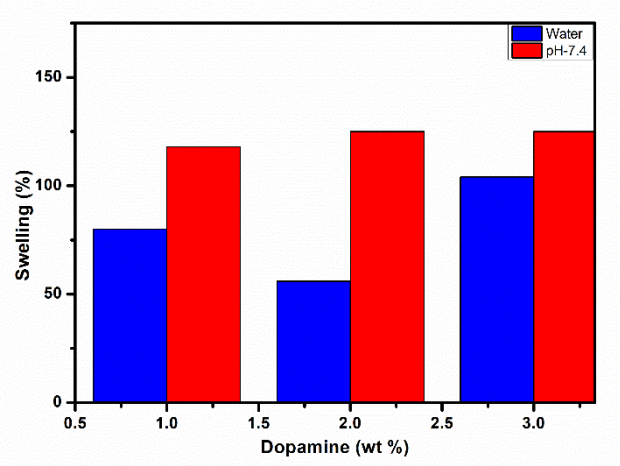

Figure 2.10 Swelling behavior of the hydrogel by varying the composition of Dopamine

2.4.11 Blood Compatibility Study

To evaluate the *in vitro* biocompatibility of synthesized hydrogel, the hemolysis test has been carried out. This test is a widely accepted method for determining the hemocompatibility of hydrogel. As shown in Figure 2.11, the hydrogel shows very little hemolysis of 4.79%. This value is within the permissible limit of 5%. Thus, this established the biocompatible nature of the hydrogel and hence is suitable for its application as biomaterials.

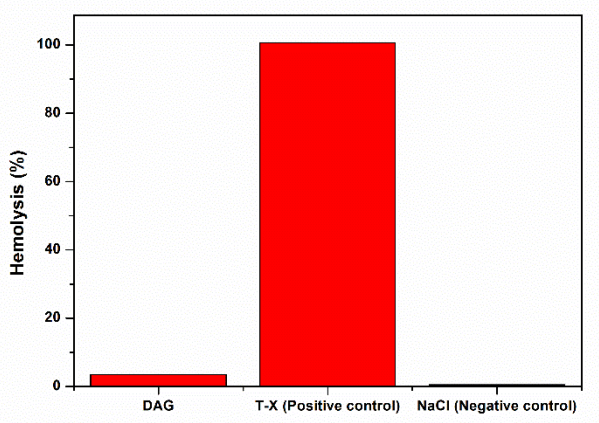

Figure 2.11 Haemolysis percentage study of the hydrogel

2.5 Conclusion

Here, in this Chapter, inspired by nature, we have successfully developed an efficient way to synthesize biocompatible hydrogel-based adhesive. This hydrogel shows excellent adhesion to diverse surfaces under both dry and wet conditions. The simple design strategy applied here allows us to eliminate the use of metal ions and other toxic additives and oxidizing agents. Here, the well-balanced combination of both covalent and non-covalent bonds provides the hydrogel with superior mechanical properties and reversible and, self-healing attributes. Unlike, other previously synthesized single-use hydrogels, this adhesive hydrogel can be repeatedly used on various surfaces and can be easily peeled off without leaving any residue. Moreover, by monitoring the swelling behavior of the hydrogel, it was found that contrary to the traditional hydrogel, the synthesized gel swells only to a limited percentage which proves to be highly advantageous for its application in biomedical fields. Again, the hemolysis test shows that the hydrogel is biocompatible. In summary, we can say that the synthesized hydrogel being adhered to different inorganic and organic surfaces under both dry and wet conditions emerges to be a potential bioadhesive for diverse medical applications such as wound dressing, tissue adhesive, actuators, biosensors, and drug delivery.

References

[1] Xie, L., Gong, L., Zhang, J., Han, L., Xiang, L., Chen, J., Liu, J., Yan, B. and Zeng, H. A wet adhesion strategy via synergistic cation–π and hydrogen bonding interactions of antifouling zwitterions and mussel-inspired binding moieties. Journal of Materials Chemistry A, 7(38):21944-21952, 2019.

[2] Majumder, A., Sharma, A. and Ghatak, A. A bioinspired wet/dry microfluidic adhesive for aqueous environments. Langmuir, 26(1):521-525, 2010.

[3] Yi, H., Lee, S.H., Seong, M., Kwak, M.K. and Jeong, H.E. Bioinspired reversible hydrogel adhesives for wet and underwater surfaces. Journal of Materials Chemistry B, 6(48):8064-8070, 2018.

[4] Ahn, B.K. Perspectives on mussel-inspired wet adhesion. Journal of the American Chemical Society, 139(30):10166-10171, 2017.

[5] Stewart, R.J., Ransom, T.C. and Hlady, V. Natural underwater adhesives. Journal of Polymer Science Part B: Polymer Physics, 49(11):757-771, 2011.

[6] Li, Y., Cheng, J., Delparastan, P., Wang, H., Sigg, S.J., DeFrates, K.G., Cao, Y. and Messersmith, P.B. Molecular design principles of Lysine-DOPA wet adhesion. Nature communications, 11(1):3895, 2020.

[7] Li, Y. and Cao, Y. The molecular mechanisms underlying mussel adhesion. Nanoscale Advances, 1(11):4246-4257, 2019.

[8] Wang, Z., Guo, L., Xiao, H., Cong, H. and Wang, S. A reversible underwater glue based on photo-and thermo-responsive dynamic covalent bonds. Materials Horizons, 7(1):282-288, 2020.

[9] Ma, Y., Zhang, B., Frenkel, I., Zhang, Z., Pei, X., Zhou, F. and He, X. Mussel-inspired underwater adhesives-from adhesion mechanisms to engineering applications: a critical review. Progress in Adhesion and Adhesives, 6:739-759, 2021.

[10] Mehdizadeh, M., Weng, H., Gyawali, D., Tang, L. and Yang, J. Injectable citrate-based mussel-inspired tissue bioadhesives with high wet strength for sutureless wound closure. Biomaterials, 33(32):7972-7983, 2012.

[11] Fan, C., Fu, J., Zhu, W. and Wang, D.A. A mussel-inspired double-crosslinked tissue adhesive intended for internal medical use. Acta Biomaterialia, 33:51-63, 2016.

[12] Lee, H., Scherer, N.F. and Messersmith, P.B. Single-molecule mechanics of mussel adhesion. Proceedings of the National Academy of Sciences, 103(35):12999-13003, 2006.

[13] Wang, X., Si, Y., Zheng, K., Guo, X., Wang, J. and Xu, Y. Mussel-inspired tough double network hydrogel as transparent adhesive. ACS Applied Polymer Materials, 1(11):2998-3007, 2019.

[14] Kim, B.J., Oh, D.X., Kim, S., Seo, J.H., Hwang, D.S., Masic, A., Han, D.K. and Cha, H.J. Mussel-mimetic protein-based adhesive hydrogel. Biomacromolecules, 15(5):1579-1585, 2014.

[15] Choi, Y.C., Choi, J.S., Jung, Y.J. and Cho, Y.W. Human gelatin tissue-adhesive hydrogels prepared by enzyme-mediated biosynthesis of DOPA and Fe^{3+} ion crosslinking. Journal of Materials Chemistry B, 2(2):201-209, 2014.

[16] Shen, M., Li, L., Sun, Y., Xu, J., Guo, X. and Prud'homme, R.K. Rheology and adhesion of poly (acrylic acid)/laponite nanocomposite hydrogels as biocompatible adhesives. Langmuir, 30(6):1636-1642, 2014.

[17] Wang, K., Hao, Y., Wang, Y., Chen, J., Mao, L., Deng, Y., Chen, J., Yuan, S., Zhang, T., Ren, J. and Liao, W. Functional hydrogels and their application in drug delivery, biosensors, and tissue engineering. International Journal of Polymer Science, 2019(1):3160732, 2019.

[18] Zhao, Q., Mu, S., Long, Y., Zhou, J., Chen, W., Astruc, D., Gaidau, C. and Gu, H. Tannin-tethered gelatin hydrogels with considerable self-healing and adhesive performances. Macromolecular materials and engineering, 304(4):1800664, 2019.

[19] Jung, H., Kim, M.K., Lee, J.Y., Choi, S.W. and Kim, J. Adhesive hydrogel patch with enhanced strength and adhesiveness to skin for transdermal drug delivery. Advanced Functional Materials, 30(42):2004407, 2020.

[20] Lee, B.P., Dalsin, J.L. and Messersmith, P.B. Synthesis and gelation of DOPA-modified poly (ethylene glycol) hydrogels. Biomacromolecules, 3(5):1038-1047, 2002.

[21] Gowda, A.H., Bu, Y., Kudina, O., Krishna, K.V., Bohara, R.A., Eglin, D. and Pandit, A. Design of tunable gelatin-dopamine based bioadhesives. International journal of biological macromolecules, 164:1384-1391, 2020.

[22] Brubaker, C.E. and Messersmith, P.B. Enzymatically degradable mussel-inspired adhesive hydrogel. Biomacromolecules, 12(12):4326-4334, 2011.

[23] Li, L., Smitthipong, W. and Zeng, H. Mussel-inspired hydrogels for biomedical and environmental applications. Polymer Chemistry, 6(3):353-358, 2015.

[24] Han, L., Lu, X., Liu, K., Wang, K., Fang, L., Weng, L.T., Zhang, H., Tang, Y., Ren, F., Zhao, C. and Sun, G. Mussel-inspired adhesive and tough hydrogel based

on nanoclay confined dopamine polymerization. ACS nano, 11(3):2561-2574, 2017.

[25] Han, L., Yan, L., Wang, K., Fang, L., Zhang, H., Tang, Y., Ding, Y., Weng, L.T., Xu, J., Weng, J. and Liu, Y. Tough, self-healable and tissue-adhesive hydrogel with tunable multifunctionality. NPG Asia Materials, 9(4):e372-e372 , 2017.

[26] Wilker, J.J. Sticky when wet. Nature Materials, 13(9):849-850, 2014.

[27] Chen, W., Wang, R., Xu, T., Ma, X., Yao, Z., Chi, B.O. and Xu, H., 2017. A mussel-inspired poly (γ-glutamic acid) tissue adhesive with high wet strength for wound closure. Journal of Materials Chemistry B, 5(28):5668-5678, 2017.

[28] Anirudhan, T.S. and Mohan, A.M. Novel pH switchable gelatin based hydrogel for the controlled delivery of the anti cancer drug 5-fluorouracil. RSC Advances, 4(24):12109-12118, 2014.

[29] Cohen, B., Pinkas, O., Foox, M. and Zilberman, M. Gelatin–alginate novel tissue adhesives and their formulation–strength effects. Acta Biomaterialia, 9(11):9004-9011, 2013.

[30] Das Purkayastha, M., Das, S., Manhar, A.K., Deka, D., Mandal, M. and Mahanta, C.L. Removing antinutrients from rapeseed press-cake and their benevolent role in waste cooking oil-derived biodiesel: conjoining the valorization of two disparate industrial wastes. Journal of Agricultural and Food Chemistry, 61(45):10746-10756, 2013.

[31] Cencer, M., Liu, Y., Winter, A., Murley, M., Meng, H. and Lee, B.P. Effect of pH on the rate of curing and bioadhesive properties of dopamine functionalized poly (ethylene glycol) hydrogels. Biomacromolecules, 15(8):2861-2869, 2014.

[32] Salomäki, M., Marttila, L., Kivelä, H., Ouvinen, T. and Lukkari, J. Effects of pH and oxidants on the first steps of polydopamine formation: a thermodynamic approach. The Journal of Physical Chemistry B, 122(24):6314-6327, 2018.

[33] Wei, Q., Zhang, F., Li, J., Li, B. and Zhao, C. Oxidant-induced dopamine polymerization for multifunctional coatings. Polymer Chemistry, 1(9), pp.1430-1433.

[34] Pinnataip, R. and Lee, B.P., 2021. Oxidation chemistry of catechol utilized in designing stimuli-responsive adhesives and antipathogenic biomaterials. Acs Omega, 6(8):5113-5118, 2010.

[35] Narkar, A.R., Kelley, J.D., Pinnaratip, R. and Lee, B.P. Effect of ionic functional groups on the oxidation state and interfacial binding property of catechol-based adhesive. Biomacromolecules, 19(5):1416-1424, 2017.

[36] Dong, Y., Zhao, S., Lu, W., Chen, N., Zhu, D. and Li, Y., 2021. Preparation and characterization of enzymatically cross-linked gelatin/cellulose nanocrystal composite hydrogels. RSC Advances, 11(18), pp.10794-10803.

[37] Das, M.P., Suguna, P.R., Prasad, K.A.R.P.U.R.A.M., Vijaylakshmi, J.V. and Renuka, M. Extraction and characterization of gelatin: a functional biopolymer. International Journal of Pharmacy and Pharmaceutical Sciences, 9(9):239, 2017.

[38] Rao, P., Sun, T.L., Chen, L., Takahashi, R., Shinohara, G., Guo, H., King, D.R., Kurokawa, T. and Gong, J.P. Tough hydrogels with fast, strong, and reversible underwater adhesion based on a multiscale design. Advanced Materials, 30(32):1801884, 2018.

[39] Zheng, Z., Bian, S., Li, Z., Zhang, Z., Liu, Y., Zhai, X., Pan, H. and Zhao, X. Catechol modified quaternized chitosan enhanced wet adhesive and antibacterial properties of injectable thermo-sensitive hydrogel for wound healing. Carbohydrate Polymers, 249:116826, 2020.

[40] Yan, Y., Xu, S., Liu, H., Cui, X., Shao, J., Yao, P., Huang, J., Qiu, X. and Huang, C. A multi-functional reversible hydrogel adhesive. Colloids and Surfaces A: Physicochemical and Engineering Aspects, 593:124622, 2020.

[41] Liang, Y., Zhao, X., Hu, T., Chen, B., Yin, Z., Ma, P.X. and Guo, B. Adhesive hemostatic conducting injectable composite hydrogels with sustained drug release and photothermal antibacterial activity to promote full-thickness skin regeneration during wound healing. Small, 15(12):1900046, 2019.

[42] Montazerian, H., Baidya, A., Haghniaz, R., Davoodi, E., Ahadian, S., Annabi, N., Khademhosseini, A. and Weiss, P.S. Stretchable and bioadhesive gelatin methacryloyl-based hydrogels enabled by in situ dopamine polymerization. ACS Applied Materials & Interfaces, 13(34):40290-40301, 2021.